Time resolved characterization of a free-burning argon arc after ignition by optical emission spectroscopy (published, see [1])

Shuiliang Ma [a,b], Hongming Gao [a], and Lin Wu [a]

[a] *State Key Laboratory of Advanced Welding Production Technology, Harbin Institute of Technology, Harbin 150001, People's Republic of China*
[b] *Plasma Research Laboratory, Australian National University, Canberra ACT 0200, Australia*

Abstract

Time resolved properties of a free-burning argon arc after ignition have been characterized using optical spectroscopic method. After ignition, when the arc current keeps constant, the plasma temperature decreases with time at any position of the arc. The decrease of the plasma temperature is associated with the increase of the arc cathode surface temperature. It is suggested that the variation of the cathode surface temperature, which changes the current density distribution over the cathode surface, leads to the decrease of the plasma temperature in the free-burning arc after ignition.

Arc plasmas have been widely used in industrial areas, such as welding, cutting, spraying, and waste treatment [2,3]. In order to control and improve these applications, a better understanding of the physical processes occurring in the plasma, especially in the cathode region, is important, which requires the plasma properties to be characterized.

Over the past few decades, a large number of studies have been devoted to such arc plasmas in both experiment [4–12] and modeling [13–17]. Using optical emission methods, arc properties, including the cathode surface temperature [4–9], the plasma temperature [6–10], and so on, have been determined and the effects of different arc conditions, e.g., the operation parameters [4,9,10], the cathode shapes and materials [5–7], have been extensively investigated. On the other hand, the recent remarkable progress in arc theory enables the electrodes, the sheath regions, and the arc plasma to be included in arc models [15,16], and thus quantitative understanding of the phenomena in the arc plasma becomes possible. Based on these models, the arc properties under different conditions have been predicted, which are in good agreement with experimental results (see [15,16] and references therein). Both experiments and modeling have shown the important role of the cathode energy transfer on arc properties [7,8,14,17]. For example, the cathode cone angles effect the cathode surface temperature distribution and, consequently, effect the plasma temperature [7,14] and different arc cathode modes and the transitions between them are considered due to the bifurcation of energy balance problem in the cathode region [8,17].

In spite of considerable research and development, the mechanisms in the arc cathode region are still not fully understood, due partly to the multiplicity and diversity of the processes involved and their interplay and partly to the extreme conditions in this region. In the case of high current arcs, most spectroscopic measurements are limited to steady state arcs [6–10], whereas there are few cases in which the transient properties in the arc cathode region have been investigated using spectroscopic methods. The time-dependent properties can provide more information about the processes in the arc and are also important for modeling. Based on a filter spectrometer and a high-speed camera, we present observations of the temporal evolution of plasma temperatures in a free-burning arc in argon after ignition and interpret the mechanism behind this phenomenon.

The arc plasma was ignited by high-frequency pulses with a welding power supply (Fronius, MW3000) and free burning in argon at atmospheric pressure between two water-cooled electrodes. The cathode was a ceriated tungsten rod (2% Ce_2O_3 by mass, diameter 3.2 mm) ground to a conical tip with an included angel $60°$, and the anode was a copper plate situated vertically bellow the cathode with a distance of 5 mm from the cathode tip. Argon (99.9% pure) was fed from the cathode nozzle with a flow rate of 10 L/min in advance of the arc ignition to protect the cathode from oxidation and as the working gas. The arc current was 200 A, which has a fluctuation less than 0.5%.

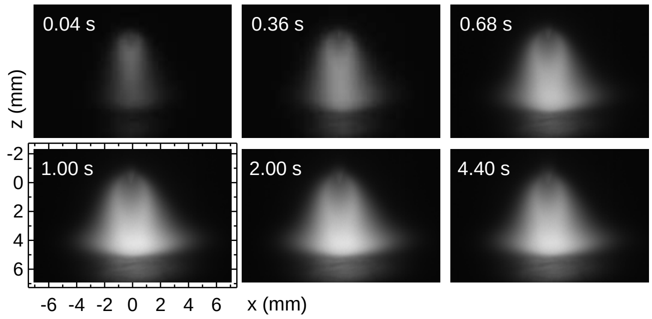

Fig. 1. A few frames of the Ar I 794.8 nm line intensity images acquired in a free-burning argon arc after ignition. The current of the arc gradually increased in steps to 200 A in 1 s time after the arc ignition and then was held constant.

Light emissions radiated from the arc were recorded with a filter spectrometer consisting of lenses and neutral-density and interference filters together with a high-speed camera (Dalsa, CA-D6-0256W). The interference filters with the center wavelength at 794.8 and 780 nm and a full width at half maximum of about 3 nm have been used for the measurement of the Ar I 794.8 nm line intensity and the near continuum radiation, respectively. The camera captures 8-bit gray images (260×260 pixels corresponding to the CCD sensor size of $2.6 \times 2.6\ \mathrm{mm}^2$) with a time resolution of 955 frames/s. The spatial resolution in the measurement is about 0.09 mm. As an example, Fig. 1 shows a few frames of the arc intensity images of the Ar I 794.8 nm line in the arc current increasing and constant stages. The arc was observed in a direction perpendicular to the x-z plane. The origin of the coordinate system was set at the cathode tip, and the positive direction of the z-axis pointed from the cathode to the anode.

Temporal evolutions of the Ar I 794.8 nm line intensity at several axial positions in the arc with distances of 0.1 to 4 mm from the cathode tip are shown in Fig. 2. In the first 1 s time after the arc was ignited, the current of the arc increased in steps gradually, which is clearly reflected from the variation of the arc intensity. After 1 s time, the arc current reached the set value 200 A and was maintained constant. However, the arc intensities at different positions of the arc varied with time: in the cathode region ($z \leq 1$ mm) there is a minor increase in

Email: shlgma@126.com (Shuiliang Ma).

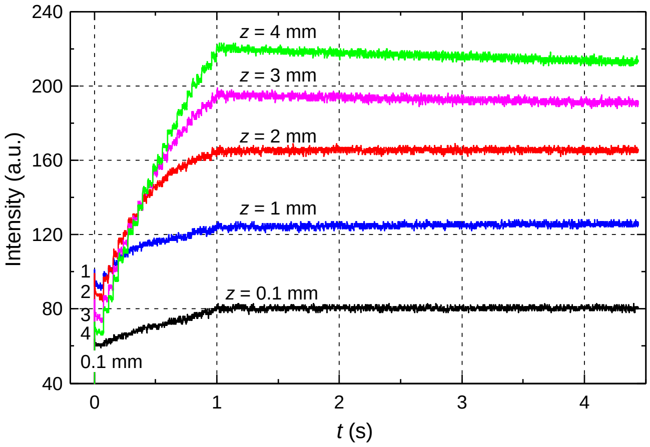

Fig. 2. Temporal evolution of the Ar I 794.8 nm line intensity at several axial positions of the 200-A free-burning arc in argon. Other conditions are the same as Fig. 1.

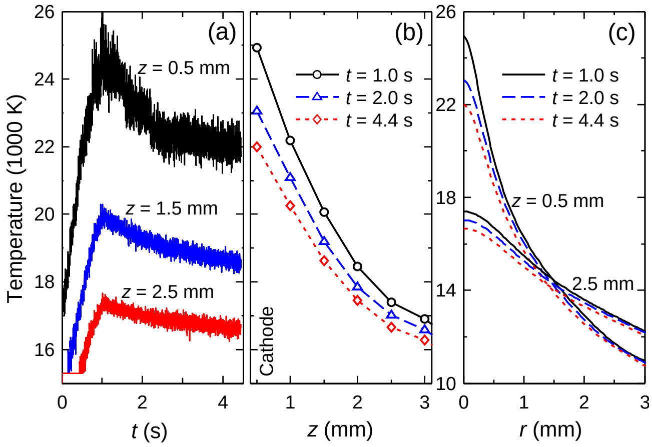

Fig. 3. Temporal, axial, and radial distributions of the plasma temperature derived based on the measured intensity images for the 200-A free-burning arc in argon, as shown in Fig. 1.

the intensity, and in regions far from the cathode ($z > 2$ mm), the intensity has a gradual decreasing trend. Since the physical conditions were kept the same during the measurement, the variation of the intensity is most likely due to the change of the arc properties.

To reconstruct the radial plasma emission coefficients, side-on measured spectral line intensity profiles were symmetrized, smoothed, and Abel inverted. Based on the assumption of local thermodynamic equilibrium (LTE), the plasma temperatures then were derived from the local emission coefficients using a modified Fowler-Milne method [18]. Fig. 3(a) shows the temporal evolution of the plasma temperature at three axial positions of the arc. At the first 1 s time after the arc was ignited, the temperature increases rapidly due to the increase of the arc current. Then, the arc current was held constant, while the temperature decreased gradually. The temperature near the cathode has the largest decreasing trend: the decrease in the temperature is about 3000 K for $z = 0.5$ mm compared with 750 K for $z = 2.5$ mm. The axial and radial distributions of the plasma temperature at three time points also show that, at any position of the arc, the temperature decreases with time (see Figs. 3(b) and (c)). The departure of the plasma from LTE cannot explain the decrease in temperature because the regions far from the cathode are usually thought of in LTE [7]. The extension of the cathode electrode due to heat expansion is also not responsible for the temperature decrease: if this is true, the temperature will increase rather than decrease with time, since the temperature in the cathode region has a much higher value. Considering all these factors and the variation of the measured intensity profiles in Fig. 2, it is believed that the plasma temperature profiles determined correctly reflect the change of the arc state.

It is difficult to determine the cathode surface condition from the measured Ar I 794.8 nm line intensities, due to the strong intensity of the arc spectral line and that reflected from the cathode. Therefore, the arc continuum radiations at 780 nm were recorded in another run with the same arc parameters. Fig. 4 shows the continuum radiation profiles along the arc axis with lateral distances of 0, 0.27, and 0.82 mm from the axis center measured at three different time points. The profiles show that, for $z < -1.2$ mm, the intensity increases with time, while, for $z > -1.2$ mm, the intensities from the cathode and from the arc both decrease with time. The axial length of the arc-cathode interaction area was found to be about 1 mm (see also [4]). Hence, the intensity at $z < -1.2$ mm can be considered due completely to the thermal radiation from the cathode surface, which indicates that the cathode surface temperature was increasing after the arc ignition. In contrast, the intensity from the arc-cathode interaction area ($z > -1.2$ mm) consists of the radiations contributed from the cathode surface and from the arc as well as the reflection by the cathode. Previous spectroscopic measurements have shown that the radiation reflected from the cathode becomes negligibly low at the cathode edge [6], thus the measured intensity in this area is due mainly to radiations from the arc and from the cathode surface. To remove the radiation from the arc, a modified Abel inversion can be used [6], which, however, will introduce large uncertainties. Considering the relatively high spatial resolution in the measurement, the intensities from the arc at two near pixels of the image should be approximately the same. Hence, the radiation at the edge of the cathode contributed from the arc can be simply removed by subtracting half of the intensity at the near pixel, which views only the light from the arc. Fig. 5 shows the temporal evolution of the intensities at six positions of the arc cathode region, as marked by the black points in Fig. 4. Points p_1 and p_4 are located at the arc axis with distances of 0.09 and 0.55 mm from the cathode tip, respectively. Points p_2 and p_5 are very close to the cathode edge, and points p_3 and p_6 are the neighbor pixels of p_2 and p_5, respectively. The deduced intensity profiles at p_2 and p_5 due to the radiation from the cathode surface are also shown in Fig. 5, as labeled by $I_2 - I_3/2$ and $I_5 - I_6/2$. These profiles indicate that the cathode surface temperatures at p_2 and p_5 were increasing after the arc ignition. Therefore, based on the variation of the radiations from the arc cathode (Figs. 4 and 5) we can conclude that the cathode surface temperature at any position increases with time in the current constant stage after the arc was ignited.

The arc cathode surface temperature is determined by the heat balance of processes, such as ohmic heating, thermal conduction in cathode bulk, thermionic cooling and heat transfer from the plasma to the cathode [7,14]. After the arc was ignited, compared with the heat loss terms, the heat inputs, including ohmic heating and heat transfer from the plasma to the cathode, are the dominant factors, thus the cathode surface temperature increases with time. The increase in the cathode surface temperature enlarges the region that contributes to the arc current by thermionic emission. Therefore, the distribution of the current density over the cathode surface expands and the maximum current density decreases. Due to the more uniformly distributed current density, the plasma temperature consequently decreases. Other experimental measurements with

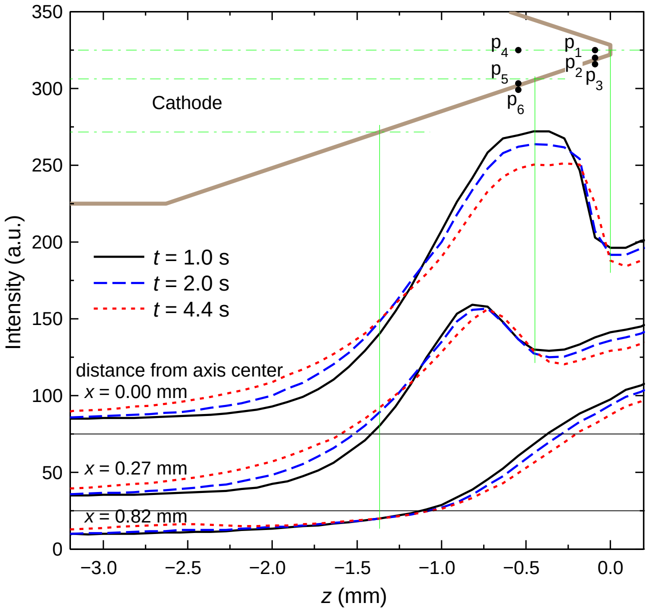

Fig. 4. Axial profiles of the plasma continuum radiation at 780 nm measured at 1.0, 2.0, and 4.4 s after the arc ignition. The dash-dotted lines in the cathode area show the positions of the axial radiation distributions with distances of 0, 0.27, and 0.82 mm from the arc axis center. The intensity profiles at different lateral positions are offset from the nearest one for clarity. The positions of the six points p_1 to p_6 are also shown.

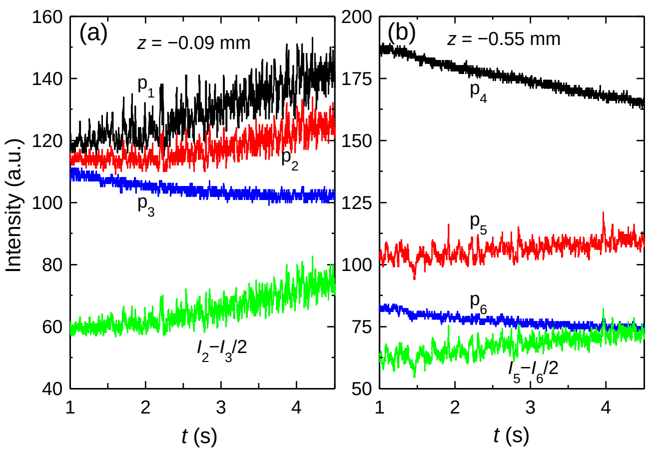

Fig. 5. Temporal evolution of the plasma continuum radiation of the 200-A free-burning arc at several cathode positions, p_1 to p_6, as shown in Fig. 4, and of the radiation emitted from the cathode surface, $I_2 - I_3/2$ and $I_5 - I_6/2$, at points p_2 and p_5, respectively, with distances from the cathode tip of -0.09 and -0.55 mm.

different cathode parameters have also demonstrated the close relationship between the plasma temperature and the cathode surface temperature [7,8] . In our case, the cathode surface temperature determines the cathode current density distribution and thus affects the plasma temperature.

In conclusion, we showed that the measured plasma temperature in a free-burning argon arc was decreasing with time after the arc ignition, which is associated with the increase of the cathode surface temperature. This phenomenon indicated the important effect of the cathode surface temperature on the plasma temperature. For further investigations, it is necessary to determine both the cathode surface temperature and current density distributions. These measurements together with modeling results will help us for a better understanding of the mechanism in the arc cathode region.

References

[1] S. Ma, H. Gao, L. Wu, Time resolved characterization of a free-burning argon arc after ignition by optical emission spectroscopy, J. Appl. Phys. 110 (2) (2011) 026102.

[2] P. Fauchais, A. Vardelle, Thermal plasmas, IEEE Trans. Plasma Sci. 25 (6) (1997) 1258–1280.

[3] P. Fauchais, A. Vardelle, Pending problems in thermal plasmas and actual development, Plasma Phys. Control. Fusion 42 (12B) (2000) B365–B383.

[4] J. A. Sillero, D. Ortega, E. Muñoz-Serrano, E. Casado, An experimental study of thoriated tungsten cathodes operating at different current intensities in an atmospheric-pressure plasma torch, J. Phys. D: Appl. Phys. 43 (18) (2010) 185204.

[5] M. Ushio, A. A. Sadek, F. Matsuda, Comparison of temperature and work function measurements obtained with different GTA electrodes, Plasma Chem. Plasma Proc. 11 (1) (1991) 81–101.

[6] J. Haidar, A. J. D. Farmer, A method for the measurement of the cathode surface temperature for a high-current free-burning arc, Rev. Sci. Instrum. 64 (2) (1993) 542–547.

[7] J. Haidar, A. J. D. Farmer, Large effect of cathode shape on plasma temperature in high-current free-burning arcs, J. Phys. D: Appl. Phys. 27 (3) (1994) 555–560.

[8] N. K. Mitrofanov, S. M. Shkol'nik, Two forms of attachment of an atmospheric-pressure direct-current arc in argon to a thermionic cathode, Tech. Phys. 52 (6) (2007) 711–720.

[9] X. Zhou, J. Heberlein, Characterization of the arc cathode attachment by emission spectroscopy and comparison to theoretical predictions, Plasma Chem. Plasma Proc. 16 (1) (1996) 229s–244s.

[10] G. N. Haddad, A. J. D. Farmer, Temperature determinations in a free-burning arc. I. Experimental techniques and results in argon, J. Phys. D: Appl. Phys. 17 (6) (1984) 1189–1196.

[11] M. E. Rouffet, Y. Cressault, A. Gleizes, J. Hlina, Thermal plasma diagnostic methods based on the analysis of large spectral regions of plasma radiation, J. Phys. D: Appl. Phys. 41 (12) (2008) 125204.

[12] B. Pokrzywka, S. Pellerin, K. Musiol, F. Richard, J. Chapelle, Observations of electric arc cathode region, J. Phys. D: Appl. Phys. 29 (1996) 2841–2849.

[13] A. Gleizes, J. J. Gonzalez, P. Freton, Thermal plasma modelling, J. Phys. D: Appl. Phys. 38 (9) (2005) R153–R183.

[14] L. E. Cram, A model of the cathode of a thermionic arc, J. Phys. D: Appl. Phys. 16 (9) (1983) 1643–1650.

[15] A. B. Murphy, M. Tanaka, S. Tashiro, T. Sato, J. J. Lowke, A computational investigation of the effectiveness of different shielding gas mixtures for arc welding, J. Phys. D: Appl. Phys. 42 (11) (2009) 115205.

[16] M. Tanaka, K. Yamamoto, S. Tashiro, K. Nakata, E. Yamamoto, K. Yamazaki, K. Suzuki, A. B. Murphy, J. J. Lowke, Time-dependent calculations of molten pool formation and thermal plasma with metal vapour in gas tungsten arc welding, J. Phys. D: Appl. Phys. 43 (43) (2010) 434009.

[17] M. S. Benilov, Understanding and modelling plasma–electrode interaction in high-pressure arc discharges: a review, J. Phys. D: Appl. Phys. 41 (2008) 144001.

[18] S. Ma, H. Gao, L. Wu, Modified Fowler–Milne method for the spectroscopic determination of thermal plasma temperature without the measurement of continuum radiation, Rev. Sci. Instrum. 82 (1) (2011) 013104.